Hindawi
Journal of Nanomaterials
Volume 2018, Article ID 5479605, 5 pages
https://doi.org/10.1155/2018/5479605

Research Article

Effect of Photoillumination on Gold-Nanoparticle-Assisted Chemical Etching of Silicon

Ming-Hua Shiao,[1] Chou-Pu Lai,[2] Bo-Huei Liao,[1] and Yung-Sheng Lin[2]

[1]*Instrument Technology Research Center, National Applied Research Laboratories, Hsinchu, Taiwan*
[2]*Department of Chemical Engineering, National United University, Miaoli, Taiwan*

Correspondence should be addressed to Yung-Sheng Lin; linys@nuu.edu.tw

Received 3 May 2018; Accepted 9 July 2018; Published 28 August 2018

Academic Editor: Achim Trampert

Metal-assisted chemical etching (MacEtch) has attracted considerable attention for its ability to fabricate micro- and nanostructures with high aspect ratios and its applications in other microelectromechanical fields. However, few studies have reported the effect of photoillumination on MacEtch. In this study, gold nanoparticles (GNPs) were deposited on the surface of a Si wafer by using the fluoride-assisted galvanic replacement reaction, and then, the effect of photoillumination on the MacEtch of the Si wafer was investigated. The etched depth increased linearly with etching time from 0–45 min and was considerably larger in the illuminated area than the nonilluminated area. A lag time was observed for the MacEtch of the nonilluminated area. However, no lag time was observed in the illuminated area. The trapping of light by the GNPs on the Si substrate surface during the MacEtch process enhanced the etching efficiency due to localized surface plasmon resonance.

1. Introduction

Metal-assisted chemical etching (MacEtch) has attracted increasing attention in recent years [1–6]. MacEtch is a simple and low-cost process for the fabrication of various Si nanostructures. The MacEtch process can also be used to control the orientation of Si nanostructures (e.g., nanowires and pores) [7]. Additionally, MacEtch can be employed to manufacture microstructures and nanostructures with high aspect ratios and is used to obtain antireflection structures, nanowires, and devices with other microelectromechanical applications [8, 9].

Metal nanoparticles (NPs) push optics beyond the diffraction limit and are thus playing a crucial role in the emerging technological revolution [10]. In comparison with bulk materials, NPs possess unique physical and chemical properties, and their nanostructures have attracted considerable attention. For example, nanoparticles of metals such as silver and gold are commonly investigated because they strongly absorb incident light [11, 12].

Metal NPs are used in applications such as solar cells [13], bioassays, and biosensing because they exhibit localized surface plasmon resonance (LSPR) [14, 15]. The shape and size of metal NPs affects their surface polarization, which in turn influences their spectral properties [15–17]. The various shapes and sizes of NPs mean that their LSPR absorption spectrum can be tailored as required. Because of localized field amplification, the excitation of surface plasmons in metal NPs deposited on a semiconductor can enhance the optical absorption of incident photons within the semiconductor region near each nanoparticle [18].

Few studies have investigated the effect of photoillumination on the MacEtch process. In this study, gold nanoparticles (GNPs) were deposited using the fluoride-assisted galvanic replacement reaction (FAGRR) onto the surface of a Si wafer. The GNP-deposited Si (GNP/Si) was characterized, and the photoillumination enhancement of the MacEtch of Si is discussed in the following sections.

2. Materials and Methods

2.1. Preparation and Characterization of GNP/Si. An n-type, single side, polished Si wafer was used as the substrate. The wafer was cut into segments of $1.5 \times 1.5\ \mathrm{cm}^2$ and washed with acetone. The Si substrate was then immersed in a mixture

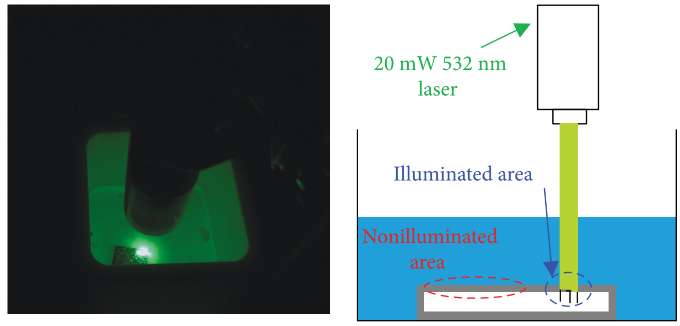

(a) (b)

Figure 1: Experimental setup: (a) top view of the real system; (b) side-view schematic.

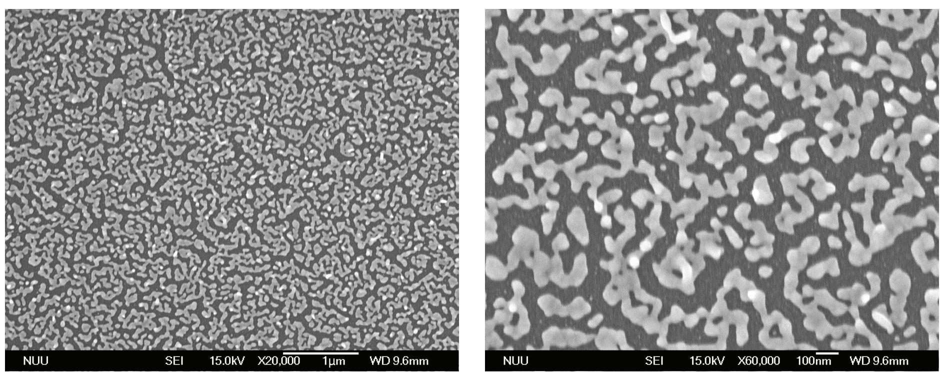

(a) (b)

Figure 2: Scanning electron microscopy (SEM) images of the gold nanoparticles (GNPs): (a) 20,000x and (b) 60,000x.

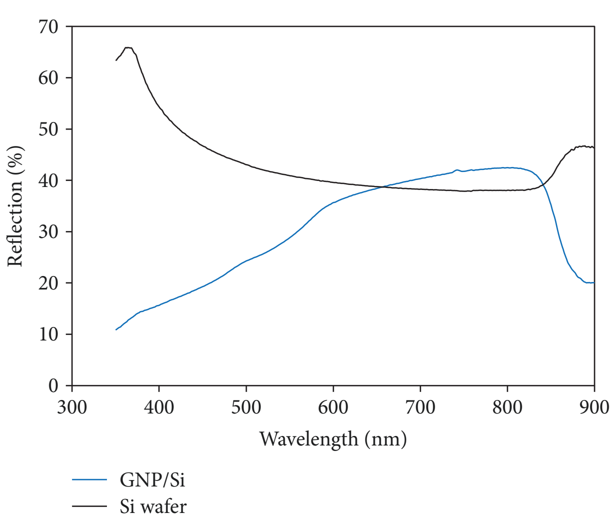

Figure 3: Reflection of the prepared GNP-deposited Si (GNP/Si) and a blank Si wafer.

comprising 240 μL of 1 M chloroauric acid ($HAuCl_4$), 8 mL of buffered oxide etchant (BOE) solution containing NH_4F and HF (UR-Reagent BOE, Uni-Onward Corp., Taiwan), and 16 mL of ultrapure water for the deposition of GNPs onto the surface of the Si substrate by using the FAGRR [19–21]. After 2 seconds of GNP deposition, the Si substrate was removed from the mixture, washed with ultrapure water, purged with nitrogen gas, and then baked at 120°C in an oven for 5 min.

The morphology of the prepared GNP/Si was observed using scanning electron microscopy (SEM) (S-4300, Hitachi, Japan). The optical reflection of the GNP/Si was studied using ultraviolet-visible spectroscopy (U-3900/3900H, Hitachi, Japan).

2.2. Photoilluminated MacEtch. The GNP/Si sample was immersed in a mixture of 10 mL of BOE solution and 10 mL of 0.46 M H_2O_2 solution. A 532 nm laser with 20 mW of power was used to illuminate the GNP/Si sample during enhanced MacEtch. Figure 1(a) displays a photograph of the actual experimental setup, and Figure 1(b) displays a schematic of the MacEtch apparatus with and without illumination in different areas of the GNP/Si sample. The incident laser beam was focused into the illuminated area, and the etching time was 60 min. When the process was completed, the etched sample was washed ultrasonically with methanol, acetone, and ultrapure water for 5 min. The drying and baking processes were the same as in the preparation of the GNP/Si sample.

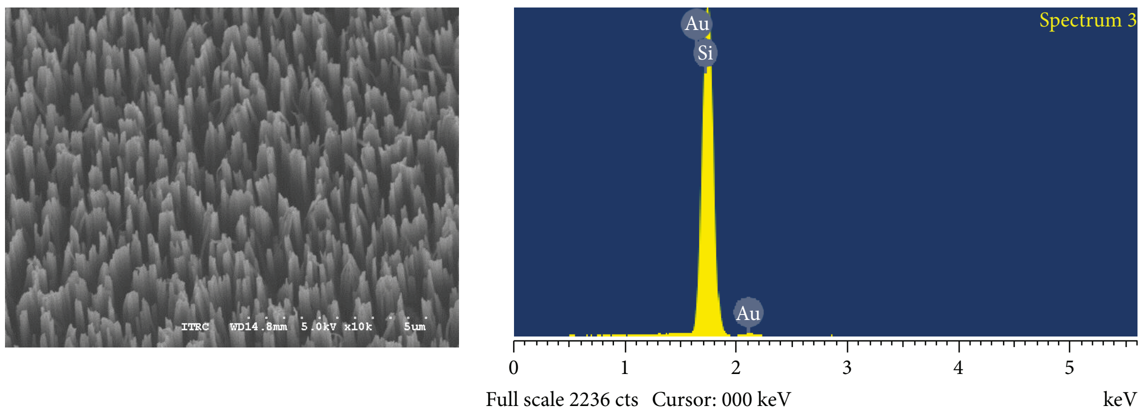

(a) (b)

Figure 4: Metal-assisted chemical etching (MacEtch) of the photoilluminated sample under an etching time of 15 min: (a) top-view SEM image and (b) energy-dispersive X-ray spectrum.

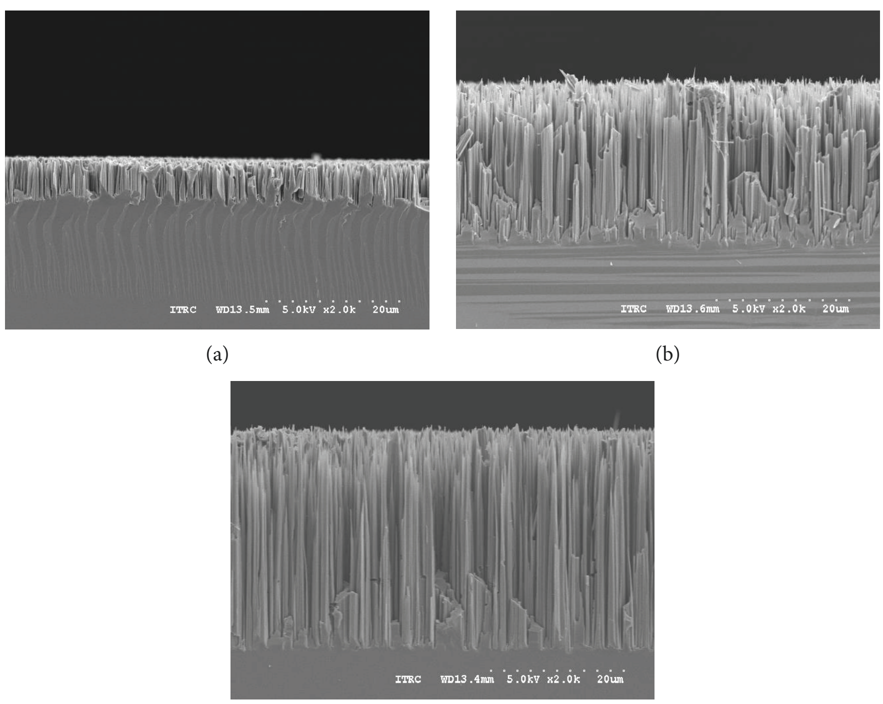

(a) (b) (c)

Figure 5: SEM images of the photoilluminated MacEtch-processed samples with GNPs. The etching times were (a) 5, (b) 25, and (c) 35 min.

3. Results and Discussion

3.1. GNP Morphology. A top-view SEM image of the GNPs deposited on the Si substrate is displayed in Figure 2. The average particle size was approximately 50 nm, and many particles fused together to form a short string. Generally, the GNPs were dispersed uniformly on the Si substrate surface, which facilitated the obtainment of a uniform pattern from the MacEtch process.

3.2. Reflection Spectrum of GNP/Si. Figure 3 displays the reflection spectrum of the GNP/Si sample and a blank Si wafer in the wavelength region of 350–900 nm. The results indicate that the GNP/Si sample reflected less light than the blank Si wafer, except in the wavelength range of 650–850 nm. Furthermore, at wavelengths of less than 800 nm, the less reflection of the GNPs/Si sample indicates higher absorption. The surface plasmon absorption of spherical GNPs depends on their size. A 50 nm GNP has maximum absorption at approximately 532 nm [16]. Therefore, in this study, a 532 nm laser was selected to demonstrate the effects of photoillumination on the MacEtch of GNPs.

3.3. Effect of Photoillumination on MacEtch. Figure 4(a) displays a top-view SEM image of a photoilluminated

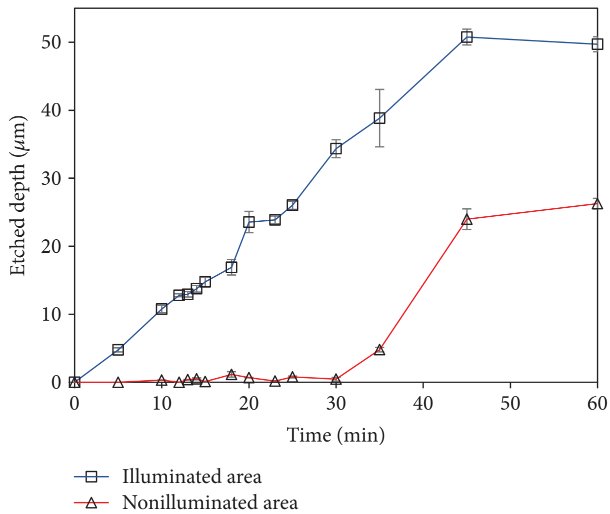

Figure 6: Etched depth for different etching times in the GNP/Si sample.

MacEtch-processed sample. The etched nanoholes were located uniformly on the Si surface. Figure 4(b) displays the energy-dispersive X-ray spectrum, which indicates that the prepared sample was clear and contained only Au and Si. No residues of the etching solutions were found on the prepared sample.

Figure 5 displays the side view of the photoilluminated MacEtch-processed samples obtained for different etching times. The results indicated that the etched depth was constant throughout the Si substrate and that the bottoms of the nanoholes were almost on the same horizontal plane. The etched depth increased with etching time. A high aspect ratio was observed for the samples obtained with an etching time of 35 min. Figure 6 illustrates the relationship between etched depth and etching time in the nonilluminated and illuminated regions. For etching times of 30 min and less, only marginal etching occurred in the nonilluminated area. After this lag time, the etched depth increased with the etching time. In the illuminated area, however, the etched depth was approximately proportional to the etching time from 0–45 min. The largest etched depth was 50 μm for the illuminated area. The etched depth was larger in the illuminated area than in the nonilluminated area. The light trapping of GNPs on the surface of the Si substrate during the MacEtch process enhanced the etching efficiency due to LSPR [22, 23]. The gas bubble which might be a gaseous phase of the etchant found in the illuminated area corresponded to the high temperature of the LSPR of the GNPs. The etched depth after 60 min nearly the same in the illuminated area resulted from the equilibrium between longitudinal etching and surface etching. The longitudinal etching rate slowed down at the later etching time because of the consumption of etchant and gas barrier for etchant transport. This result in this study was in agreement with the enhanced optical absorption due to surface plasmon excitation in semiconductors that was observed in one study using extinction spectroscopy [18].

4. Conclusions

Metal-assisted chemical etching was a simple and low-cost process for the fabrication of various Si nanostructures. The effect of photoillumination on the GNP-assisted chemical etching of silicon was investigated in this study. In the illuminated region, the etched depth in the Si wafer increased with the etching time. Conversely, only marginal etching occurred on the Si surface in the nonilluminated area during a 30 min lag time. The enhancement of the MacEtch process achieved using photoillumination was attributed to the trapping of light by the GNPs on the Si substrate surface, which improved the etching efficiency.

Abbreviations

BOE:	Buffered oxide etchant
FAGRR:	Fluoride-assisted galvanic replacement reaction
GNPs:	Gold nanoparticles
GNP/Si:	GNP-deposited Si
LSPR:	Localized surface plasmon resonance
MacEtch:	Metal-assisted chemical etching.

Data Availability

Previously reported reflectance spectra data were used to support this study and are available at doi:10.3390/nano8050282. This prior study is cited at the relevant place within the text as reference [22].

Conflicts of Interest

The authors declare no conflict of interest. The founding sponsors had no role in the design of the study; collection, analyses, and interpretation of the data; writing of the manuscript; and decision to publish the results.

Authors' Contributions

Ming-Hua Shiao and Yung-Sheng Lin conceived and designed the experiments; Chou-Pu Lai and Bo-Huei Liao performed the experiments; Ming-Hua Shiao and Yung-Sheng Lin analyzed the data; and Yung-Sheng Lin wrote the paper.

Acknowledgments

The authors are grateful to Ms. Nancy Chu from the Instrument Technology Research Center, National Applied Research Laboratories, for her assistance with the SEM analyses. This work was supported by the Ministry of Science and Technology, Taiwan (Contract nos.: 105-2221-E-492-003-MY2 and 106-2221-E-239-022).

References

[1] K. Peng, A. Lu, R. Zhang, and S. T. Lee, "Motility of metal nanoparticles in silicon and induced anisotropic silicon etching," *Advanced Functional Materials*, vol. 18, no. 19, pp. 3026–3035, 2008.

[2] M. Zahedinejad, S. D. Farimani, M. Khaje, H. Mehrara, A. Erfanian, and F. Zeinali, "Deep and vertical silicon bulk micromachining using metal assisted chemical etching," *Journal of Micromechanics and Microengineering*, vol. 23, no. 5, article 055015, 2013.

[3] H. Han, Z. Huang, and W. Lee, "Metal-assisted chemical etching of silicon and nanotechnology applications," *Nano Today*, vol. 9, no. 3, pp. 271–304, 2014.

[4] F. Toor, J. B. Miller, L. M. Davidson et al., "Nanostructured silicon via metal assisted catalyzed etch (MACE): chemistry fundamentals and pattern engineering," *Nanotechnology*, vol. 27, no. 41, p. 412003, 2016.

[5] L. Romano, J. Vila-Comamala, K. Jefimovs, and M. Stampanoni, "Effect of isopropanol on gold assisted chemical etching of silicon microstructures," *Microelectronic Engineering*, vol. 177, pp. 59–65, 2017.

[6] L. U. Vinzons, L. Shu, S. P. Yip, C.-Y. Wong, L. L. H. Chan, and J. C. Ho, "Unraveling the morphological evolution and etching kinetics of porous silicon nanowires during metal-assisted chemical etching," *Nanoscale Research Letters*, vol. 12, no. 1, p. 385, 2017.

[7] Z. Huang, N. Geyer, P. Werner, J. de Boor, and U. Gösele, "Metal-assisted chemical etching of silicon: a review," *Advanced Materials*, vol. 23, no. 2, pp. 285–308, 2011.

[8] B. Wu, A. Kumar, and S. Pamarthy, "High aspect ratio silicon etch: a review," *Journal of Applied Physics*, vol. 108, no. 5, article 051101, 2010.

[9] A. Backes, A. Bittner, M. Leitgeb, and U. Schmid, "Influence of metallic catalyst and doping level on the metal assisted chemical etching of silicon," *Scripta Materialia*, vol. 114, pp. 27–30, 2016.

[10] M. Pelton, J. Aizpurua, and G. Bryant, "Metal-nanoparticle plasmonics," *Laser & Photonics Review*, vol. 2, no. 3, pp. 136–159, 2008.

[11] J. Z. Zhang and C. Noguez, "Plasmonic optical properties and applications of metal nanostructures," *Plasmonics*, vol. 3, no. 4, pp. 127–150, 2008.

[12] W. Hou and S. B. Cronin, "A review of surface plasmon resonance-enhanced photocatalysis," *Advanced Functional Materials*, vol. 23, no. 13, pp. 1612–1619, 2013.

[13] R. Lu, L. Xu, Z. Ge et al., "Improved efficiency of silicon nanoholes/gold nanoparticles/organic hybrid solar cells via localized surface plasmon resonance," *Nanoscale Research Letters*, vol. 11, no. 1, p. 160, 2016.

[14] K. A. Willets and R. P. Van Duyne, "Localized surface plasmon resonance spectroscopy and sensing," *Annual Review of Physical Chemistry*, vol. 58, no. 1, pp. 267–297, 2007.

[15] E. Petryayeva and U. J. Krull, "Localized surface plasmon resonance: nanostructures, bioassays and biosensing—a review," *Analytica Chimica Acta*, vol. 706, no. 1, pp. 8–24, 2011.

[16] S. Link and M. A. El-Sayed, "Shape and size dependence of radiative, non-radiative and photothermal properties of gold nanocrystals," *International Reviews in Physical Chemistry*, vol. 19, no. 3, pp. 409–453, 2000.

[17] M. Hu, C. Novo, A. Funston et al., "Dark-field microscopy studies of single metal nanoparticles: understanding the factors that influence the linewidth of the localized surface plasmon resonance," *Journal of Materials Chemistry*, vol. 18, no. 17, pp. 1949–1960, 2008.

[18] D. M. Schaadt, B. Feng, and E. T. Yu, "Enhanced semiconductor optical absorption via surface plasmon excitation in metal nanoparticles," *Applied Physics Letters*, vol. 86, no. 6, article 063106, 2005.

[19] C. Carraro, R. Maboudian, and L. Magagnin, "Metallization and nanostructuring of semiconductor surfaces by galvanic displacement processes," *Surface Science Reports*, vol. 62, no. 12, pp. 499–525, 2007.

[20] W. Ye, Y. Chen, F. Zhou, C. Wang, and Y. Li, "Fluoride-assisted galvanic replacement synthesis of Ag and Au dendrites on aluminum foil with enhanced SERS and catalytic activities," *Journal of Materials Chemistry*, vol. 22, no. 35, p. 18327, 2012.

[21] X. Bai, Y. Gao, and L. Zheng, "Galvanic replacement mediated growth of dendritic gold nanostructures with a three-fold symmetry and their applications to SERS," *CrystEngComm*, vol. 13, no. 10, p. 3562, 2011.

[22] M. H. Shiao, C. T. Lin, J. J. Zeng, and Y. S. Lin, "Novel gold dendritic nanoforests combined with titanium nitride for visible-light-enhanced chemical degradation," *Nanomaterials*, vol. 8, no. 5, p. 282, 2018.

[23] M. H. Shiao, C. T. Lin, H. J. Huang et al., "Novel gold dendritic nanoflowers deposited on titanium nitride for photoelectrochemical cells," *Journal of Solid State Electrochemistry*, 2018.